Published online November 2, 2017

Special Section: The Root Zone: Soil Physics and Beyond

Roots Partially in Contact with Soil: Analytical Solutions and Approximation in Models of Nutrient and Water Uptake

Peter de Willigen, Marius Heinen,* and Meine van Noordwijk

Root–soil contact entails a trade-off between uptake opportunities and aeration requirements. A single root in the center of a cylinder of soil has been the standard geometry for which most root-level water and nutrient uptake models have been derived. However, this implies assumptions about complete root–soil contact and regularly spaced, parallel roots that do not conform to the situation in the field. In reality, the frequency distribution of transport distances will differ from what the cylinder model assumes, both by partial root–soil contact and irregular three-dimensional (3-D) distribution. We derived analytical equations describing the transport of water and nutrients to and uptake by roots in partial contact with soil for two extremes: (i) part of each root in contact or (ii) part of all roots in full contact and the rest without. Solutions range from negligible impacts to proportionality of uptake to the part of roots in contact with soil.

Core Ideas

- Partial root–soil contact has an impact on uptake.
- For the radial situation, a steady-rate solution can be used.
- For partial longitudinal contact, steady-rate solutions cannot always be used.

Abbreviations: 3-D, three-dimensional; lr, partial longitudinal root–soil contact; pde, partial differential equation; pr, partial radial root–soil contact.

P. de Willigen and M. Heinen, Wageningen Environmental Research, Wageningen, the Netherlands; M. van Noordwijk, World Agroforestry Centre (ICRAF), Bogor, Indonesia, and Plant Production Systems, Wageningen Univ. and Research, Wageningen, the Netherlands. *Corresponding author (marius.heinen@wur.nl).

Received 16 Mar. 2017.
Accepted 18 June 2017.

Citation: de Willigen, P., M. Heinen, and M. van Noordwijk. 2017. Roots partially in contact with soil: Analytical solutions and approximation in models of nutrient and water uptake. Vadose Zone J. doi:10.2136/vzj2017.03.0060

Single-root models consider the soil in a cylindrical perspective with roots at the center and assume local homogeneity of the soil matrix. Empirical diffusion coefficients correct for the changes in path length when soils dry out and less pore space is effectively involved (Nye and Tinker, 1977). A complementary view starts at a random position in 3-D belowground space and assumes that transport of water or nutrients will be directed toward the root that generates the strongest concentration gradients, most likely the nearest active root. Common procedures for delineating these in two-dimensional cross-sections of soil are based on a nearest-neighbor Dirichlet tessellation (de Willigen and van Noordwijk, 1987b) and implicitly assume full root–soil contact and roots growing perpendicular to the plane of observation. Root distribution and root–soil contact in the field, however, depend on the way roots interact with soil aggregates and pores (Altemüller and Haag, 1983; van Noordwijk et al., 1993a; Kooistra and van Noordwijk, 1996). Contact between roots and soil is one of the critical issues for progress in soil science as identified by Bouma (2010). While models aimed at quantifying soil–plant relations at the field scale will necessarily have to make simplifying assumptions at the single-root level, the level of bias introduced into standard single-root models by oversimplifying the geometry of the root–soil interface remains a concern. How serious the bias is may depend primarily on the level of compensation that can exist within a root system where individual roots face a range of circumstances. This study dealt with more realistic, complex root–soil geometries and derived ways in which the simple cylindrical model can still be used with appropriate adjustments.

Most models describe water uptake by plants as demand driven, where the demand is driven by atmospheric conditions. In contrast, models for nutrient uptake have a long history of describing supply-driven, concentration-dependent uptake rates, only indirectly accounting for the feedback in the plant that downregulates uptake to meet demand. This difference may be due to the fact that it is easier to measure total uptake of water rather than nutrients on a daily basis. Where the Baldwin et al. (1973), Nye and Tinker (1977), and Claassen and Barber (1974) models of nutrient uptake started with concentration-dependent uptake and steady-state solutions for transport in the soil, de Willigen and van

Noordwijk (1987a, 1994a, 1994b) presented analytical solutions for the steady-rate situation that can emerge where demand-driven uptake per unit root is constant in time. Given a constant uptake requirement, the demand per unit root length is inversely proportional to root-length density, and the root-length density required to match supply and demand depends on the demand as well as the nutrient pool in the soil (Fig. 1). Point Y compared with X in this figure indicates the increase in root-length density in a given soil needed to compensate for a 50% decrease in soil supply, while Z compared with X indicates that a similar increase in root-length density is needed to meet a doubled demand on the same soil.

Roots need sufficient direct contact with air-filled macropores to meet their aeration requirements (Bartholomeus et al., 2008), as modeled for radial transport by de Willigen and van Noordwijk (1984) and van Noordwijk and de Willigen (1984) and for longitudinal transport by de Willigen and van Noordwijk (1989). On the other hand, roots need to be in contact with the water-filled micro- and mesopores of the soil to take up water and nutrients, with direct contact with the solid phase accounting for only a small part of the total nutrient uptake (Jenny and Grossenbacher, 1963). The required compromise of intermediate values of root–soil contact can explain the concept of optimal soil compaction: in a soil that is too loosely packed, root–soil contact and unsaturated hydraulic conductivity are low, whereas in a very dense soil, penetration resistance and root aeration are limiting root growth and functioning (Kooistra et al., 1992; Veen et al., 1992). Moderate soil compaction offers some benefits to growing roots by increasing root–soil contact, facilitating uptake (Tracy et al., 2011). Eight out of 17 woody species from Mediterranean ecosystems tested had higher total biomass with moderate degrees of soil compaction, possibly a result of increased root–soil contact (Alameda and Villar, 2009). Optimal soil structure in the field differs among crops (Arvidsson and Håkansson, 2014) in ways that reflect this compromise and differential abilities of crops to develop internal longitudinal aeration

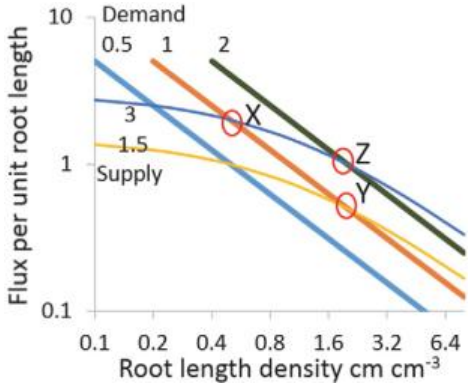

Fig. 1. Schematic relationship between potential uptake (supply) and demand per unit root length as a function of root-length density (logarithmic scales). Point Y compared with X in this figure indicates the increase in root-length density in a given soil needed to compensate for a 50% decrease in soil supply, while Z compared with X indicates that a similar increase in root-length density is needed to meet a doubled demand on the same soil.

inside roots once the root tip has penetrated (van Noordwijk and Brouwer, 1993). Root tips rotating when they reach voids, as studied by Darwin (1888), can find aggregate surfaces, and root hairs help them to attach to such, leading to a complex 3-D partial root contact situation in the field (van Noordwijk et al., 1993a; Fig. 2).

The various complexities of actual root–soil geometry, including details of root–soil contact, can be approached by developing transport models for specified geometries or by a generic method that seeks approximate solutions based on transport-distance equivalent representations (de Willigen and van Noordwijk, 1987a, 1987b; Rappoldt, 1992; van Noordwijk, 1992; van Noordwijk et al., 1993b). However, while 3-D root representations can be reduced to a frequency distribution of two-dimensional (cylindrical) models once characterized by the transport distances involved, current methods for doing so (Fig. 2E and 2F) critically depend on an assumption of complete contact at the root–soil interface. Dunbabin et al. (2013) compared features of six current 3-D models and the progress they allow in relating soil and root hydraulic properties to wetting and drying phases of a soil profile but found that none of them deals with the dynamics of root–soil contact. De Willigen et al. (2012) compared four root water uptake routines of different complexity (one-, two-, and three-dimensional) that are all embedded in soil–water balance models. The models differed in the way they handle compensation in wetter layers for reduced uptake opportunities in drier ones, with consequences for hydraulic redistribution in the soil. Both soil physical and root physiological factors were found to be important for proper deterministic modeling of root water uptake, but uncertainly remains on how variable root–soil contact can best be included in one-, two-, or three-dimensional models.

The two-dimensional sampling of root–soil contact on thin sections of soil allows the root contact percentage to be quantified as well as the angle with which roots intersect the plane of observation (van Noordwijk et al., 1992); this observation method can test the homogeneity in the root distribution as well as qualitatively infer the fraction of roots that grow in cracks, biogenic macropores, or those that penetrate into aggregates with full soil contact for as long as they stay inside such aggregate. Thin-section observations can complement what can be directly observed and mapped on profile walls (Han et al., 2015; van Noordwijk et al., 2000). In situ endoscopy visualizes the response of crop roots to biopores (Kautz and Köpke, 2010; Athmann et al., 2013). The average widths measured with a digital camera for the root–soil air gap for black locust (*Robinia pseudoacacia* L.) in open fields and in a root growth chamber were 0.24 and 0.39 mm, respectively (Liu et al., 2015). Root–soil contact can now be measured using X-ray microtomography with accuracy on the contact area within 2.5% (Schmidt et al., 2012). Soil close to roots, the rhizosphere, not only has chemical and biological properties that are significantly different from those of soil located some distance away but may also differ in a physical sense, as root penetration implies local compaction by changes in particle and aggregate packing (Young, 1998; Schmidt

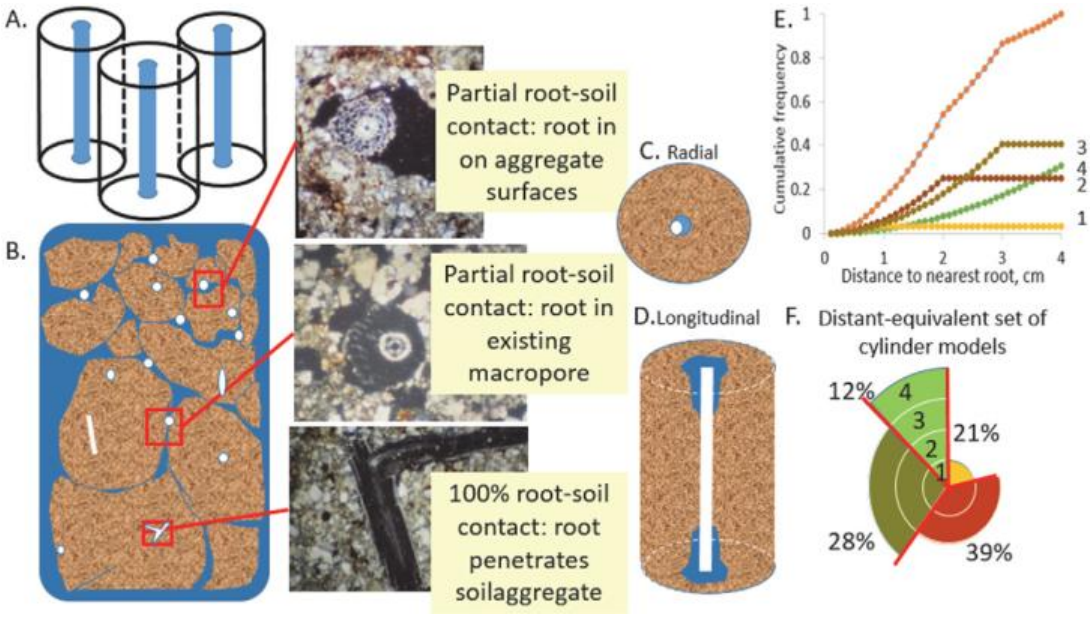

Fig. 2. Aspects of the soil–root geometry in the field that deviate from (A) the regular cylinder model, (B) with root–soil contact varying from 0 to 100% in thin-section samples, and partial root–soil contact that can be interpreted in (C) radial and (D) longitudinal directions; (E) characterizing the cumulative frequency distribution of soil to the nearest root distance can be used to (F) derive equivalent sets of cylinder models.

et al., 2012). In a study of wheat (*Triticum aestivum* L.) roots in southern Australia, White and Kirkegaard (2010) found that 30 to 40% of topsoil roots were clumped within pores and cracks, increasing to 85 to 100% in the subsoil (>0.6 m). Wheat roots clumped into pores contacted the surrounding soil via numerous root hairs, whereas roots in cracks were appressed to the soil surface and had very few root hairs. Approximately 85% of all roots observed in biopores in the field by Athmann et al. (2013) established contact with the pore wall. The direct physical role of root hairs in anchoring root tips during soil penetration was studied by Bengough et al. (2016) by use of hairless maize (*Zea mays* L.) mutants compared with wild-type plants. Hairless seedlings took 33 h to anchor themselves compared with 16 h for wild-type roots in 1.2 g cm^{-3} soil, but there was no significant advantage of root hairs in the densest soil (1.5 g cm^{-3}). In a comparison of barley (*Hordeum vulgare* L.) genotypes with and without root hairs, a role for root hairs in P uptake in low-strength soil was found but not in high-strength soil, probably the result of support for root penetration and improved root–soil contact (Haling et al., 2013).

Partial root–soil contact may be needed under wet soil conditions to aerate plant roots, but root–soil contact decreases and air-filled gaps emerge in dry soil when roots shrink (Liu et al., 2015; Carminati et al., 2013). In a study with lupin (*Lupinus albus* L.), part of the roots maintained contact with the soil via hydrated mucilage, while others (transport roots) had air-filled gaps and a hydrophobic rhizosphere, which isolate roots from the soil and may limit (hydraulic equilibration) water loss to dry soil (Carminati and Vetterlein, 2013). Hydraulic equilibration occurs especially at night when concurrent aboveground water demand for transpiration is low; estimates of the amount of water involved range from a few percentage points to a substantial part of the daily demand (Bayala et al., 2008; Neumann and Cardon, 2012) while also prolonging the life span of fine roots, rewetting the rhizosphere with consequences for nutrient mobility, and maintaining root–soil contact in dry soils. The dynamics of root–soil contact in drying soil have received specific attention since Herkelrath et al. (1977) suggested that shrinkage of roots and air-filled gaps can cause a major resistance in the soil–plant–atmosphere continuum. Faiz and Weatherley (1978) confirmed that shaking pots with sunflower (*Helianthus annuus* L.) plants in early stages of water stress could increase water uptake, presumably by reestablishing root–soil contact. Current understanding is that such gaps indeed are observable in the field (Liu et al., 2015) but that their role as a primary hindrance to uptake remains contested (Carminati et al., 2013). The presence of root hairs is a major plant adaptation to keep such a situation from developing (North and Nobel, 1997; Haling et al., 2013; Bengough et al., 2016). Hydraulic redistribution of water through roots can, however, maintain roots turgid and in contact with drying soil as long as water is accessible elsewhere in the root system (Bayala et al., 2008).

In this study, we addressed two questions for two extremes for partial root–soil contact:

1. Can the analytical steady-rate solutions for nutrient and water uptake be adjusted, given cylinder geometry, to partial root–soil contact effects in either radial (part of each root in contact; Fig. 2C) or longitudinal (part of all roots is in full contact, the rest without; Fig. 2D) representations?

2. Is there a simple expression for the additional root-length density needed in a layer of soil to account for the more complex

root–soil geometry through use of the standard model but with adjusted effective root-length density?

Model

Basic Situation

The starting point for our discussions on nutrient uptake (de Willigen and van Noordwijk, 1987a) is the uptake as generated by plant demand, that is, the rate of dry-matter production times the required nutrient content. Uptake by the roots is assumed to be in accordance with plant demand as long as transport in the soil can maintain the concentration at the root surface above a certain limiting concentration. This limiting concentration is virtually zero for most conditions found in agricultural practice (de Willigen and van Noordwijk, 1987a, Table 3.2 and Section 3.4) Physiological experiments suggest that the limiting concentrations are on the order of 100, 10, and 1 μmol L^{-1} for N, K, and P, respectively, with equivalent amounts of available nutrients on the order of 3.5, 10.5, and 7.8 to 78 kg ha^{-1}. For N and K, this is <5% of what a soil needs to contain for good crop growth; for P on soils with high adsorption constants, it may represent a non-negligible amount.

Nutrient demand of agricultural crops during a major part of the growing season can be taken to be constant (van Noordwijk et al., 1990). For the conditions chosen here, this also means a constant uptake rate per root, each root being confined to an equal volume of soil. The uptake potential of such a root can be characterized by a characteristic time: the period during which the concentration at the root surface exceeds the limiting (in practice zero) concentration or, to put it differently, the period during which uptake is in accordance with plant demand. This characteristic time is called the period of unconstrained uptake and is indicated here as T_u (d) or t_u (dimensionless units).

The steady-rate solutions shown below are valid for linear and nonlinear (e.g., Langmuir type) adsorption and for water uptake provided the limiting value of concentration is reached when the steady-rate phase applies. In the case of water, instead of concentration the matric flux potential is substituted.

Some doubts could be raised as to the validity of the approach for the scale considered here—a root radius of 0.025 cm and transport distances of 0.25 to 0.5 cm. As stated by Metselaar and van Lier (2011), the Darcy length L_D is on the order of 0.02 to 0.3 cm. Therefore, 0.02 cm is the minimum transport length required to apply the Darcy equation. The transport distances mentioned above are larger. Because of partial contact, however, there is heterogeneity in the flow field. If we apply the aforementioned criterion to the length of the root circumference partaking in uptake, the condition is then $\alpha 2\pi R_0 > L_D$, where α is the degree of contact and R_0 is the radius of the root. With the root radius applied here, this means that α is >0.13, and this is about the minimum value we used.

Partial Differential Equations and Boundary Conditions

Solute

The partial differential equation (pde) describing transport of solute has the general form as follows:

$$\frac{\partial B}{\partial T} = -\vec{\nabla}\cdot\vec{V}C + \vec{\nabla}\cdot D\vec{\nabla}C \qquad [1]$$

where B is the bulk density of the solute (mg cm^{-3}), T is time (d), C is the concentration in the soil solution (mg mL^{-1}), V s the volume flux of the soil solution (cm d^{-1}), and D is the diffusion coefficient (cm^2 d^{-1}). It is to be understood that the bulk density is mass per unit volume of soil and concentration is mass per unit volume of soil solution. The situation we deal with is that of a cylindrical root at the center of a soil cylinder. The root is supposed to be a member of a collection of uniformly distributed roots with length L (cm) and radius R_0 (cm). If the root-length density is given by L_{rv} (cm cm^{-3}), the radius R_1 (cm) of the soil cylinder is

$$R_1 = \frac{1}{\sqrt{\pi L_{rv}}} \qquad [2]$$

From the assumed geometry, it follows that the condition at the outer boundary is that of vanishing flux **F**:

$$R = R_1, \quad |\mathbf{F}| = 0 \qquad [3]$$

The condition at the root surface is that of constant flux generated by constant demand of the plant. If the demand amounts to A (mg cm^{-2} d^{-1}), each root has to take up at a rate of A/L_{rv} (mg d^{-1}). The boundary condition at that part of the root surface that partakes in uptake is

$$R = R_0, \quad \alpha S|\mathbf{F}| = -\frac{A}{L_{rv}} \qquad [4]$$

where S is the root surface (cm^2) and α is the fraction in contact with soil. For the remaining part of the surface, the flux is zero:

$$R = R_0, \quad (1-\alpha)S|\mathbf{F}| = 0 \qquad [5]$$

Two situations are considered: one where there is contact over the total length of the root but over a part of its radial surface, and the other is contact over the total radial surface and over a part of the longitudinal surface. The two situations are depicted in Fig. 2. The geometry of the root–soil system makes it preferable to express the equations in cylindrical coordinates R (the radial coordinate), ψ (the tangential coordinate), and Z (the vertical coordinate taken positive downward). In the case of partial radial contact no gradients in Z will occur, and likewise for partial longitudinal contact no gradients in ψ will occur. To simplify notation, dimensionless variables and parameters will be used. In the derivations for

nutrient transport, we restrict ourselves to transport by diffusion. For the two situations, the set of equations are as follows.

Radial Partial Root–Soil Contact.

This situation is depicted in Fig. 3. The partial differential equation in dimensionless form is

$$\frac{\partial b}{\partial t}=\frac{1}{r}\frac{\partial}{\partial r}r\frac{\partial c}{\partial r}+\frac{1}{r^2}\frac{\partial^2 c}{\partial \psi^2} \quad [6]$$

where $b = B/B_i$, the initial bulk density; $c = C/C_i$, the initial concentration; $r = R/R_0$, and $t = DT/{R_0}^2$, where D is the diffusion coefficient and T is time. The symbols used are also explained in Table 1. The boundary conditions are given by

$$\begin{aligned} &r=1, \quad 0<\psi<\psi_1, \quad \frac{\partial c}{\partial r}=-\frac{\pi\omega}{\psi_1}\\ &r=1, \quad \psi_1<\psi<\pi, \quad \frac{\partial c}{\partial r}=0\\ &r=\rho, \quad 0<\psi<\pi, \quad \frac{\partial c}{\partial r}=0 \end{aligned} \quad [7]$$

where $\rho = R_1/R_0$, $\omega = -\rho^2/(2\phi\eta)$, with $\phi = DC_i/(AR_0)$ is a supply–demand parameter, $\eta = L/R_0$, and R_1 is given in Eq. [2]. The boundary condition at the root surface (where $r = 1$) states that at the part in contact with soil, given by the contact angle ψ_1, the required uptake is a factor π/ψ_1 larger than the uptake in the case of complete contact to satisfy the demand of the crop.

Longitudinal Partial Root–Soil Contact.

The partial differential equation is

$$\lambda^2\frac{\partial b}{\partial t}=\frac{\lambda^2}{r}\frac{\partial}{\partial r}r\frac{\partial c}{\partial r}+\frac{\partial^2 c}{\partial z^2} \quad [8]$$

where $z = \pi Z/L$, $\lambda = L/(\pi R_0)$ and the boundary conditions become

$$\begin{aligned} &r=1, \quad 0<z<z_0, \quad \frac{\partial c}{\partial r}=0\\ &r=1, \quad z_0<z<z_1, \quad \frac{\partial c}{\partial r}=-\frac{\pi\omega}{z_1-z_0}\\ &r=1, \quad z_1<z<\pi, \quad \frac{\partial c}{\partial r}=0\\ &r=\rho, \quad 0<z<\pi, \quad \frac{\partial c}{\partial r}=0 \end{aligned} \quad [9]$$

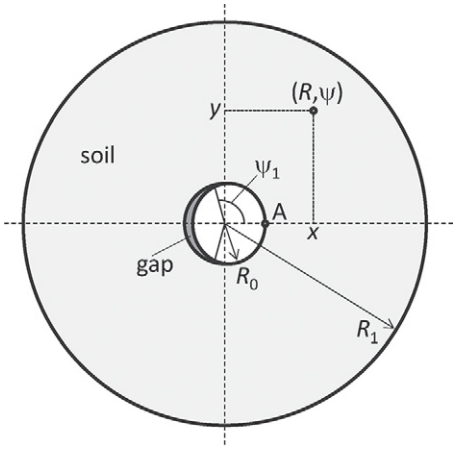

Fig. 3. Schematic representation of a root in a soil cylinder; the position of any point in the soil is given by polar (R,ψ) or Cartesian (X,Y) coordinates; the degree of contact is given by the angle ψ_1.

Water

For water, the pde is similar to that of solute, the bulk density of soil water is now given as water content θ (mL cm^{-3}), the transport coefficient k is the hydraulic conductivity (cm d^{-1}), and the total head is equivalent to the concentration. The pde thus is

$$\frac{\partial\theta}{\partial T}=\vec{\nabla}\cdot k\vec{\nabla}H \quad [10]$$

where H is the sum of the pressure head h (cm) and the gravitational potential Z (cm):

Table 1. List of symbols.

Symbol	Name	Dimension	Dimensionless symbol
R_0	root radius	cm	–
D	diffusion coefficient	cm^2 d^{-1}	–
T	time	d	$t = DT/{R_0}^2$
T_u	period of unconstrained uptake	d	$t_u = DT_u/{R_0}^2$
R	radial coordinate	cm	$r = R/R_0$
R_1	radius soil cylinder	cm	$\rho = R_1/R_0$
Z	vertical coordinate	cm	$z = \pi Z/L$
ψ	tangential coordinate	–	–
L	root length	cm	$\eta = L/R_0$, $\lambda = L/(\pi R_0)$
2S	root surface	cm^2	–
C_i	initial concentration	mg mL^{-1}	–
C	concentration	mg mL^{-1}	$c = C/C_i$
A	uptake rate nutrient	mg cm^2 d^{-1}	$\omega = -\rho^2/(2\phi\eta)$
ϕ	supply/demand parameter	–	$\phi = DC_i/(AR_0)$
B_i	initial bulk density	mg cm^{-3}	–
B	bulk density of solute	mg cm^{-3}	$b = B/B_i$
θ_i	initial water content	mL cm^{-3}	–
θ	water content	mL cm^{-3}	–
E_{pot}	potential transpiration rate	cm d^{-1}	$\upsilon = \rho^2 E_{pot}/2\eta$
α	fractional contact between root and soil	–	–
β	buffer capacity	mL cm^{-3}	–
h	pressure head	cm	–
H	total head	cm	–
k	conductivity	cm d^{-1}	–

$$H = h - Z \qquad [11]$$

The boundary condition for the part of the root surface in contact with the soil is (see Eq. [4])

$$R = R_0, \quad \alpha S|\mathbf{F}| = -\frac{E_p}{L_{rv}} \qquad [12]$$

where E_p is the potential transpiration (mL cm^{-2} d^{-1} = cm d^{-1}). The other boundary conditions are identical to those shown in Eq. [3] and [5].

An important difference between the transport of solute and that of water is that in the latter case the flux is nonlinear, that is, the conductivity is a nonlinear function of pressure head, whereas the solute diffusion coefficient is independent of concentration. By defining the matric flux potential Φ (cm^2 d^{-1}) (Raats, 1970) as

$$\Phi = \int k\,dh, \text{ so that } k\nabla h = \nabla\Phi$$

the relevant equations get a simpler form, as shown below.

Partial Radial Root–Soil Contact (pr)

$$\frac{\partial\theta}{\partial T} = \frac{1}{R}\frac{\partial}{\partial R}R\frac{\partial\Phi}{\partial R} + \frac{1}{R^2}\frac{\partial^2\Phi}{\partial\psi^2} \qquad [13]$$

The boundary conditions are given by

$$\begin{aligned} &r = 1, \quad 0 < \psi < \psi_1, \quad \frac{\partial\Phi}{\partial r} = -\frac{\pi\upsilon}{\psi_1} \\ &r = 1, \quad \psi_1 < \psi < \pi, \quad \frac{\partial\Phi}{\partial r} = 0 \\ &r = \rho, \quad 0 < \psi < \pi, \quad \frac{\partial\Phi}{\partial r} = 0 \end{aligned} \qquad [14]$$

where

$$\upsilon = \frac{\rho^2 E_{pot}}{2\eta}$$

Partial Longitudinal Root–Soil Contact (lr)

$$\lambda^2\frac{\partial\theta}{\partial t} = \frac{\lambda^2}{r}\frac{\partial}{\partial r}r\frac{\partial\Phi}{\partial r} + \frac{\partial^2\Phi}{\partial z^2} \qquad [15]$$

The boundary conditions become

$$\begin{aligned} &r = 1, \quad 0 < z < z_0, \quad \frac{\partial\Phi}{\partial r} = 0 \\ &r = 1, \quad z_0 < z < z_1, \quad \frac{\partial\Phi}{\partial r} = -\frac{\pi\upsilon}{z_1 - z_0} \\ &r = 1, \quad z_1 < z < \pi, \quad \frac{\partial\Phi}{\partial r} = 0 \\ &r = \rho, \quad 0 < z < \pi, \quad \frac{\partial\Phi}{\partial r} = 0 \end{aligned} \qquad [16]$$

Limiting Values. As mentioned above, the limiting concentration can be assumed to be zero. As soon as the concentration at that point of the root surface where the concentration is minimal becomes zero, the required uptake rate cannot be satisfied. For pr, the minimum is found at $r = 1$, $\psi = 0$ (Point A in Fig. 3). For lr, this point is found at either $r = 1$, $z = 0$ or $z = \pi$ in the case of asymmetrical contact area, or $z = \pi/2$ in the case where the contact area is symmetrical.

For water, however, different options for the limiting value of pressure head are possible—for example, the pressure head at the permanent wilting point. We chose a limiting value based on a relation between leaf water potential and transpiration rate proposed by Campbell (1985, 1991) as described below.

Parameter Values and Functions Used

Root Parameters. We assumed that the majority of nutrients is taken up from the plow layer with an assumed thickness of 20 cm. This then is also the root length (L). The root radius (R_0) was set at 0.025 cm. One of the goals of our study was to show the effect of root-length density (L_{rv}) so we used two values: 1 and 5 cm cm^{-3}. The corresponding radius of the soil cylinder then became 0.56 and 0.25 cm, respectively. The limiting concentration was set at zero for the reasons mentioned above.

Available Amount and Uptake Parameters. The amount of nutrients available for uptake was taken from the recommendations in the handbook of the Dutch extension service (http://www.handboekbodemenbemesting.nl): 300 and 225 kg ha^{-1} for NO_3–N and K, respectively. Nitrate is not adsorbed and K only slightly, with an adsorption constant of 10 mL cm^{-3}. The recommendation for P is based on a water extraction method, the so-called P_W number; from it and using the adsorption parameters given below, the corresponding amount in kilograms P per hectare can be calculated (van Noordwijk et al., 1990). The adsorption isotherm was described as a two-term Langmuir equation, leading to the following relation between P bulk density and concentration:

$$B_p = \frac{b_1 A_1 C}{1 + b_1 C} + \frac{b_2 A_2 C}{1 + b_2 C} + \theta C \qquad [17]$$

where θ is the soil water content set at 0.3 mL cm^{-3}. We did our calculations for two Dutch soils with widely different adsorption parameters: light sand and basin clay. The parameters are given in Table 2. Figure 4 shows the adsorption isotherm of the two soils.

Uptake parameters were based on a crop growth rate of 200 kg dry matter ha^{-1} d^{-1}, a N content of 1.5%, a K content of 0.75%, and a P content of 0.22%, which results in uptake rates of 3, 1.5, and 0.44 kg ha^{-1} d^{-1} for N, K, and P, respectively.

The uptake and supply of water are of a different character than those of nutrients. The available amount of nutrient in the soil is,

for arable crops in modern agricultural practice, on the order of the total uptake during the growing season, the length of which is ~100 d. The amount of water in the soil root zone is sufficient for a couple of weeks and is replenished by rainfall (and possibly sprinkler irrigation) during the growing season.

The limiting water content was taken as that water content where the possible uptake rate is just less than required. The actual transpiration, in our approach, is a function of the leaf water potential. The functional relation is that proposed by Campbell (1985, 1991), which has the following form:

$$\frac{E_{act}}{E_{pot}} = \frac{1}{1+\left(h/h_{1/2}\right)^n} \qquad [18]$$

where E_{act} is the actual transpiration (cm d^{-1}), E_{pot} is the potential transpiration (cm d^{-1}), h is the soil water pressure head (cm), and $h_{1/2}$ (cm) and n are parameters. The parameter values were taken from Kremer et al. (2008): $h_{1/2} = -16{,}600$ cm and $n = 7$. By assuming steady state in the root–leaf path, the pressure head at the root surface can be calculated for the case where the actual transpiration is 99% of the potential transpiration. This is the limiting value that is dependent on potential transpiration, conductance in the root-xylem–leaf-xylem path, the conductance in the root-surface–root-xylem path, the root-length density, and the degree of contact. The calculations were done for two soils taken from the Staring series (Wösten et al., 2001), a sandy soil B3 and a loamy soil B13 with different hydraulic properties (see Fig. 5).

Solutions and Results

Steady-Rate Solution

Because of the nature of the boundary conditions (constant flux at the root surface and zero flux at the outer boundary of the soil cylinder), a steady-rate situation develops, where the rate of change becomes independent of time and, in the case of transport by diffusion only, also independent of position. The steady change rate can be found from a simple balance. The decrease in the total amount of nutrient or water equals the total uptake rate:

$$\frac{\mathrm{d}}{\mathrm{d}T}\int_0^L\int_0^{2\pi}\int_{R_0}^{R_1} RB\,\mathrm{d}R\,\mathrm{d}\psi\,\mathrm{d}Z = \int_0^L\int_0^{2\pi}\int_{R_0}^{R_1} R\frac{\partial B}{\partial T}\mathrm{d}R\,\mathrm{d}\psi\,\mathrm{d}Z = -\pi R_1^2 A \qquad [19]$$

Table 2. Parameters of the two-term Langmuir equation (Eq. [17]) for two soils.

Parameter	Fine sand	Basin clay
b_1, mL mg^{-1}	500	16,000
b_2, mL mg^{-1}	8.5	130
A_1, mg cm^{-3}	0.16	0.15
A_2, mg cm^{-3}	0.19	0.49

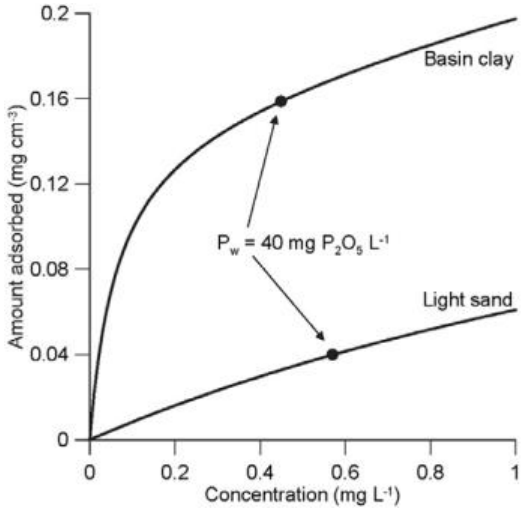

Fig. 4. Phosphorus adsorption isotherm for fine sand and basin clay; the points indicate the position of adsorbed P for a P_W number of 40 mg P_2O_5 L^{-1} soil.

By definition, steady rate implies independence of time and here, also, independence of coordinates. Then one finds, on evaluating the integral, the following:

$$\pi\left(R_1^2 - R_0^2\right)L\frac{\partial B}{\partial T} = -\pi R_1^2 A, \text{ or } \frac{\partial B}{\partial T} = -\frac{R_1^2 A}{\left(R_1^2 - R_0^2\right)L} \qquad [20]$$

In dimensionless variables, this becomes

$$\frac{\partial b}{\partial t} = \frac{2\omega}{\rho^2 - 1} \qquad [21]$$

Substitution of Eq. [19] into Eq. [1], [3], or [5] leads to a linear pde, even in the case of a nonlinear relation between b and c. The steady-rate pde can be solved using the finite cosine transform (Churchill, 1972). For the pr situation, the solution (the derivation can be found in de Willigen and van Noordwijk, 1987a) is

$$c(r,\psi,t) = 1+\omega\left[\frac{2t}{\beta\left(\rho^2-1\right)} + \frac{r^2-\rho^2}{2\left(\rho^2-1\right)} + \frac{\rho^4\ln\rho}{\left(\rho^2-1\right)^2} - \frac{\rho^2\ln r}{\rho^2-1} - \frac{1+\rho^2}{4\left(\rho^2-1\right)} + \frac{2}{\psi_1}\sum_{k=1}^{\infty}\frac{r^{2k}+\rho^{2k}}{k^2 r^k\left(\rho^{2k}-1\right)}\sin k\psi_1\cos k\psi\right] \qquad [22]$$

For the lr situation, the solution is

$$c(r,z,t) = 1+\omega\left[\frac{2t}{\beta\left(\rho^2-1\right)} + \frac{r^2-\rho^2}{2\left(\rho^2-1\right)} + \frac{\rho^4\ln\rho}{\left(\rho^2-1\right)^2} - \frac{\rho^2\ln r}{\rho^2-1} - \frac{1+\rho^2}{4\left(\rho^2-1\right)} + \frac{2\lambda}{z_1-z_0}\sum_{k=1}^{\infty}\frac{\sin kz_1 - \sin kz_0}{k^2}F(k,r)\cos kz\right] \qquad [23]$$

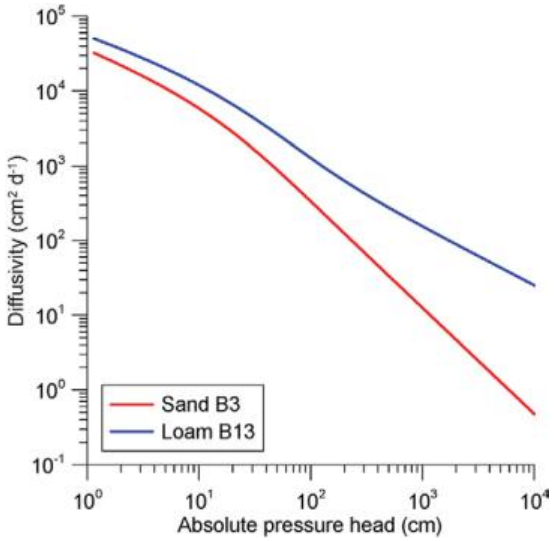

Fig. 5. The relation between diffusivity and water content for two soils from the Staring series.

$$F(k,r)=\frac{I_0(\xi r)K_1(\xi\rho)+K_0(\xi r)I_1(\xi\rho)}{I_1(\xi\rho)K_1(\xi)-K_1(\xi\rho)I_1(\xi)},\ \text{where}\ \xi=\frac{k}{\lambda}$$

The symbols I_n and K_n indicate modified Bessel functions of the first and second kind, respectively, and order n.

Period of Unconstrained Uptake

An important time parameter is the length of the period of unconstrained uptake (t_u), that is, the period during which the uptake rate equals the demand of the crop. For the situation of partial radial contact, the minimum concentration is found at Point A in Fig. 3 with coordinates $r = 1$ and $\psi = 0$. When the concentration at this point reaches the limiting value, the required uptake can no longer be maintained. The period of unconstrained uptake can accordingly be calculated by setting $c(1,0,t_u) = c_{lim} = 0$:

$$c(1,0,t_u)=0$$
$$=1+\omega\left[\frac{2t_u}{\beta(\rho^2-1)}-\frac{1}{2}+\frac{\rho^4\ln\rho}{(\rho^2-1)^2}-\frac{1+\rho^2}{4(\rho^2-1)}+\frac{2}{\psi_1}\sum_{k=1}^{\infty}\frac{\rho^{2k}+1}{k^2(\rho^{2k}-1)}\sin k\psi_1\right] \quad [24]$$

Solving Eq. [24] for t_u results in

$$t_u(\psi_1)=t_{u,max}-\beta G(\rho)-\frac{\beta(\rho^2-1)}{\psi_1}\sum_{k=1}^{\infty}\frac{\rho^{2k}+1}{k^2(\rho^{2k}-1)}\sin k\psi_1 \quad [25]$$

where $t_{u,max}$ is the dimensionless form of the maximum uptake period, that is, the total available amount divided by the required uptake:

$$t_{u,max}=\frac{\rho^2-1}{\rho^2}\phi\eta \quad [26]$$

and

$$G(\rho)=\frac{1}{2}\left(\frac{1-3\rho^2}{4}+\frac{\rho^4\ln\rho}{\rho^2-1}\right)$$

Because ρ is >10, Eq. [25] can be well approximated by

$$t_u(\psi_1)=\phi\eta-\beta\rho^2\left(\frac{\ln\rho}{2}-\frac{3}{8}\right)-\beta\rho^2\left(\frac{1}{\psi_1}\sum_{k=1}^{\infty}\frac{\sin k\psi_1}{k^2}\right) \quad [27]$$

The period of unconstrained uptake in the case of complete contact can be given similarly to Eq. [27] as

$$t_u(\pi)=\phi\eta-\frac{\beta\rho^2}{2}\left(\frac{\ln\rho}{2}-\frac{3}{8}\right) \quad [28]$$

It is convenient to express the concentration at t_u with respect to the limiting concentration at Point A in Fig. 3:

$$c(r,\psi,t_u)=\omega\left\{\frac{r^2-1}{2(\rho^2-1)}-\frac{\rho^2\ln r}{\rho^2-1}+\frac{2}{\psi_1}\sum_{k=1}^{\infty}\left[\frac{r^{2k}+\rho^{2k}}{r^k(\rho^{2k}-1)}-\frac{\rho^{2k}+1}{(\rho^{2k}-1)}\right]\times\frac{\sin k\psi_1}{k^2}(\cos k\psi-1)\right\} \quad [29]$$

For the longitudinal situation (lr), the location of the minimum concentration is, depending on the position of the contact area, either at the upper or lower end of the root surface or at the center of the contact area. The z coordinate of the minimum concentration is denoted by z_{min}, and so z_{min} can have the values 0, π, or π/2. The concentration at the point $(1, z_{min})$ and $t = t_u$ is

$$c(1,z_{min},t_u)=0$$
$$=1+\omega\left[\frac{2t_u}{\beta(\rho^2-1)}-\frac{1}{2}+\frac{\rho^4\ln\rho}{(\rho^2-1)^2}-\frac{1+\rho^2}{4(\rho^2-1)}+\frac{2\lambda}{z_1-z_0}\sum_{k=1}^{\infty}\frac{\sin kz_1-\sin kz_0}{k^2}F(k,1)\cos kz_{min}\right] \quad [30]$$

and the period of unconstrained uptake is found as

$$t_u=\phi\eta-\beta\rho^2\left(\frac{\ln\rho}{2}-\frac{3}{8}\right)-\frac{\lambda\beta\rho^2}{z_1-z_0}\sum_{k=1}^{\infty}\frac{\sin kz_1-\sin kz_0}{k^2}F(k,1)\cos kz_{min} \quad [31]$$

If $z_0 = z_{min} = 0$, Eq. [29] becomes

$$t_u(z_1)=\phi\eta-\beta\rho^2\left(\frac{\ln\rho}{2}-\frac{3}{8}\right)-\frac{\lambda\beta\rho^2}{z_1}\sum_{k=1}^{\infty}\frac{\sin kz_1}{k^2}F(k,1) \quad [32]$$

which has a lot in common with Eq. [27].

As before, a general equation for the concentration at $t = t_u$ can be obtained by giving the concentration with respect to the limiting concentration:

$$c(r,z,t_u) = \omega\left\{\frac{r^2-1}{2(\rho^2-1)} - \frac{\rho^2 \ln r}{\rho^2-1} - \frac{2\lambda}{z_1-z_0}\sum_{k=1}^{\infty}\frac{\sin kz_1 - \sin kz_0}{k^2} \times\left[F(k,r)\cos kz - F(k,1)\cos kz_{\min}\right]\right\} \quad [33]$$

Equations [27] and [32] can be used to check if the limiting value is reached before the steady-rate phase has begun. A sine qua non is, of course, that $t_u \geq 0$, but this condition is not sufficient; a stronger condition is the requirement that the maximum concentration is less than its initial value ($c = 1$). The maximum value is found at the point (ρ,π) for pr and at points (ρ,π) or $(\rho,0)$ for lr. In doing so, we found that with the parameter values used in the lr situation, the minimum concentration becomes zero before steady rate is achieved.

In the case of nonlinear adsorption, where the steady-rate solution is valid, t_u can be calculated by integration of the bulk density B calculated with Eq. [29] or [32] and the parameters of the adsorption isotherm to obtain the amount of nutrient at t_u. This amount is then subtracted from the initial amount and the result is divided by the uptake rate with t_u as a result. If the steady-rate solution cannot be used, the relevant pde is numerically integrated.

Equi-concentration Lines and Streamlines

Figures 6 and 7 show the equi-concentration lines and the streamlines for pr and lr contact, respectively. The results pertain to a nutrient that is not adsorbed by the soil, that is, $K_a = 0$, for example, for NO_3. The transport distances for pr are on the order of a few millimeters and in case of lr, on the order of a decimeter or more in the case of an asymmetric position of the contact area. This also implies that for the pr situation the steady-rate solution can be used. For the lr situation, however, the steady-rate solution cannot be used, even in the case of high fractional contact and low adsorption, so we derived the complete solution of the concentration valid for the time prior to steady rate.

Complete Solution for the Partial Longitudinal Root–Soil Contact Situation

The pde and boundary conditions are given in Eq. [8] and [9], and the initial condition is that of uniform bulk density:

$$T = 0,\quad R_0 \leq R \leq R_1,\quad 0 \leq Z \leq L,\quad B = B_i \quad [34]$$

In the case of a linear adsorption isotherm, the concentration is proportional to the bulk density:

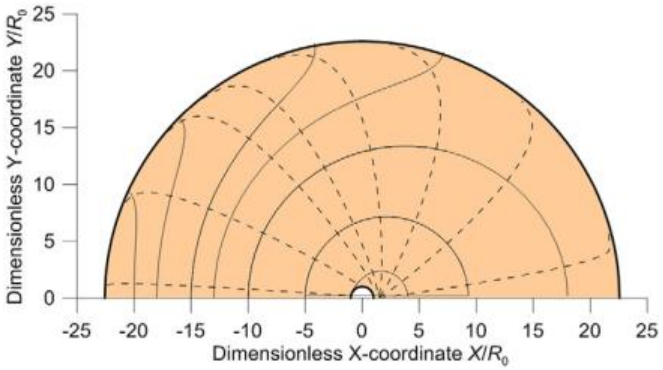

Fig. 6. Equi-concentration lines and streamlines (dashed) when steady rate is attained in the radial situation; fractional contact = 0.25, no adsorption, root-length density = 1 cm cm^{-3}, R_0 = 0.025 cm.

$$C = \frac{B}{\beta},\quad \text{where } \beta = K_a + \theta \quad [35]$$

In dimensionless symbols, the pde Eq. [8] becomes

$$\lambda^2\frac{\partial c}{\partial \tau} = \frac{\lambda^2}{r}\frac{\partial}{\partial r}r\frac{\partial c}{\partial r} + \frac{\partial^2 c}{\partial z^2},\quad \text{where } \tau = t/\beta \quad [36]$$

With the boundary conditions in Eq. [9] and the initial condition,

$$\tau = 0,\quad 1 \leq r \leq \rho,\quad 0 \leq z \leq \pi,\quad c = 1 \quad [37]$$

By applying the cosine transform and the Laplace transform, the solution could be found as (here shown in parts for subsequent explanation):

$$c =$$

$$1 + \omega\left[\frac{2\tau}{\rho^2-1} + \frac{r^2-\rho^2}{2(\rho^2-1)} + \frac{\rho^4\ln\rho}{(\rho^2-1)^2} - \frac{\rho^2\ln r}{\rho^2-1} - \frac{1+\rho^2}{4(\rho^2-1)}\right] \quad [38a]$$

$$+\pi\omega\sum_{n=1}^{\infty}\frac{J_1(\alpha_n)J_1(\rho\alpha_n)}{\alpha_n}H_0(r,\alpha_n)\exp\left(-\alpha_n^2\tau\right) \quad [38b]$$

$$+\omega\sum_{k=1}^{\infty}2p(k)\frac{I_1(\rho\xi)K_0(r\xi) + K_1(\rho\xi)I_0(r\xi)}{\xi\left[I_1(\rho\xi)K_1(\xi) - I_1(\xi)K_1(\rho\xi)\right]}\cos kz \quad [38c]$$

$$-\omega\sum_{k=1}^{\infty}2p(k)\frac{2\exp\left(-\xi^2\tau\right)}{\xi^2(\rho^2-1)}\cos kz \quad [38d]$$

$$+\omega\sum_{k=1}^{\infty}2p(k)\left\{\sum_{n=1}^{\infty}\frac{2\exp\left[-\left(\alpha_n^2+\xi^2\right)\tau\right]H_1(r,\alpha_n)}{-\left(\alpha_n^2+\xi^2\right)}\right\}\cos kz \quad [38e]$$

where

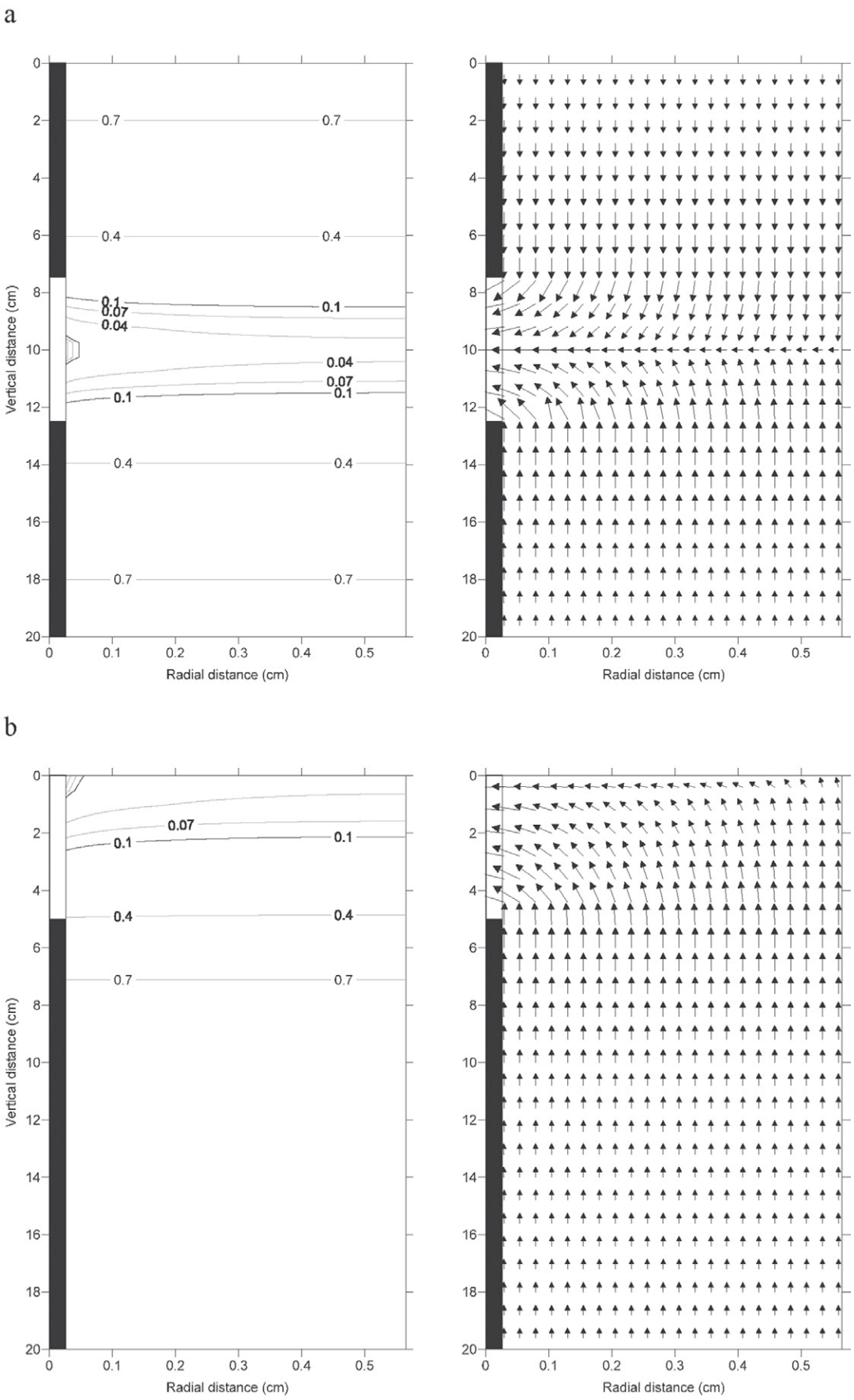

Fig. 7. Equi-concentration lines (left) and streamlines (right) in the longitudinal situation with fractional contact of 25% for (a) symmetrical and (b) asymmetrical position of contact area; fractional contact = 0.25, no adsorption, root-length density = 1 cm cm^{-3}.

$$H_0(r,\alpha_n)=\frac{Y_1(\rho\alpha_n)J_0(r\alpha_n)-J_1(\rho\alpha_n)Y_0(r\alpha_n)}{J_1^2(\alpha_n)-J_1^2(\rho\alpha_n)}$$

where α_n is the nth root of $Y_1(\rho\alpha_n)J_1(\alpha_n)-J_1(\rho\alpha_n)Y_0(\alpha_n)=0$

$$p(k)=\frac{\sin kz_1-\sin kz_0}{k(z_1-z_0)}$$

and

$$H_1=\frac{J_1(\rho\alpha)Y_0(r\alpha)-J_0(r\alpha)Y_1(\rho\alpha)}{\rho[J_1(\alpha)Y_0(\rho\alpha)-J_0(\rho\alpha)Y_1(\alpha)]+[Y_1(\rho\alpha)J_0(\alpha)-J_1(\rho\alpha)Y_0(\alpha)]}$$

Equation [38a] is the steady-rate solution for complete contact; Eq. [38a] and [38b] give the complete solution (transient and steady rate) for complete contact. Complete contact implies $z_0 = 0$ and $z_1 = \pi$ and consequently, $p(k) = 0$. Equations [38a] and [38c] give the steady-rate solution for partial contact.

Results

Figure 8 (left) shows the period of unconstrained uptake for NO_3 with a required uptake rate of 3 kg ha^{-1} d^{-1} and an available amount of 300 kg ha^{-1} and a root-length density of 1 and 5 cm cm^{-3} and for both longitudinal and radial partial contact, respectively. In the latter situation, there is practically no influence of degree of contact or root-length density; the realized uptake period is almost equal to the maximum of 100 d. This is in contrast to the longitudinal situation where the degree of contact has a strong influence on the length of the unconstrained uptake period, especially if the contact area is asymmetrically positioned. Here again, the root-length density hardly influences T_u at a fractional contact >0.5. When mass flow, generated by transpiration of 0.3 cm d^{-1} occurs, this results in an increase of 70 d of T_u.

A larger root-length density leads in our scheme to smaller transport distances radially; for instance, for an L_{rv} of 5 cm cm^{-3} the distance between the root surface and outer boundary of the soil cylinder is about half of that for an L_{rv} of 1 cm cm^{-3}. So, in the radial situation, the longest transport distance is halved. In the case of longitudinal partial contact, the longest distance is still of the order of 10 cm. To illustrate this further, Fig. 9 was constructed. It gives the difference in the period of unconstrained uptake between a root-length density of 5 and 1 cm cm^{-3} for a solute that is linearly adsorbed with an adsorption constant of 10, a required uptake of 1.5 kg ha^{-1}, and an available amount of 225 kg ha^{-1}. The difference in uptake period is, in the longitudinal situation, almost independent of fractional contact and especially at lower contact less than the difference in the radial situation.

Figure 10 shows the difference in T_u as a result of the difference in root-length density for a nutrient with nonlinear adsorption, for example, P. Above, we showed the P-adsorption isotherms (Fig. 4) for two Dutch soils (fine sand and basin clay). The adsorption isotherms of these soils differ substantially: the amount of available P at a P_W number of 40 is 318 and 80 kg ha^{-1} for basin clay and fine sand, respectively, and the average adsorption constant amounts to 354 and 70, respectively. The results shown in Fig. 8 and 9 are qualitatively the same as those for nutrients with linear adsorption; the effect of an increase in root-length density is higher for the radial than for the longitudinal partial contact.

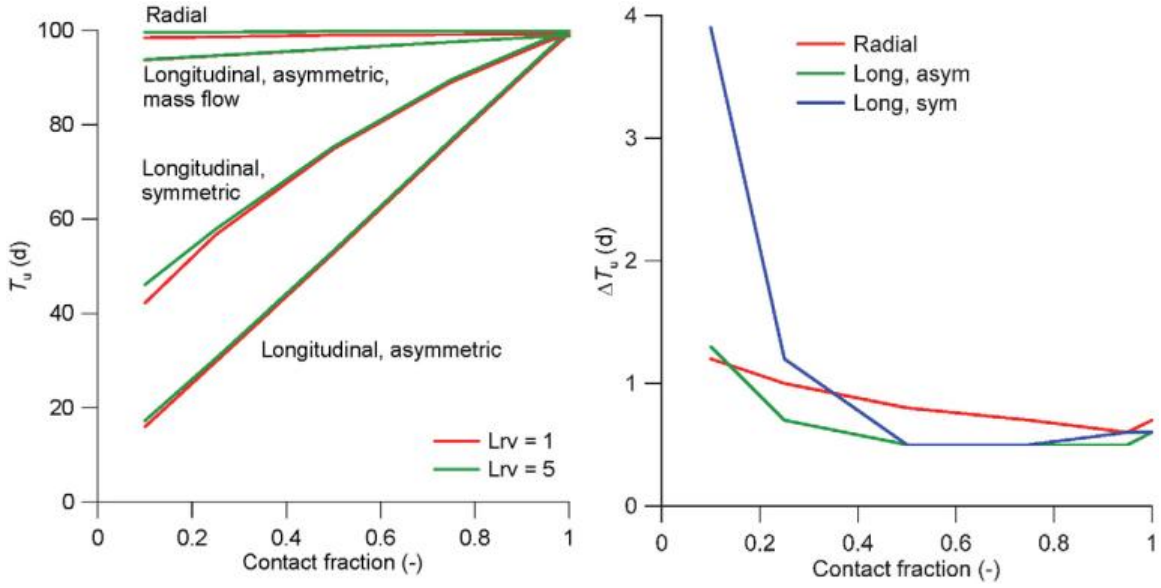

Fig. 8. The period of unconstrained uptake (T_u) of NO_3 with a required uptake rate of 3 kg ha^{-1} d^{-1} and initial available amount of 300 kg ha^{-1} for partial radial and longitudinal contact, the latter for asymmetrical and symmetrical position of contact area, as a function of the degree of partial contact, with mass flow generated by a transpiration rate of 0.3 cm d^{-1} (left) and the difference in T_u between root-length densities (L_{rv}) of 5 and 1 cm cm^{-3} (right).

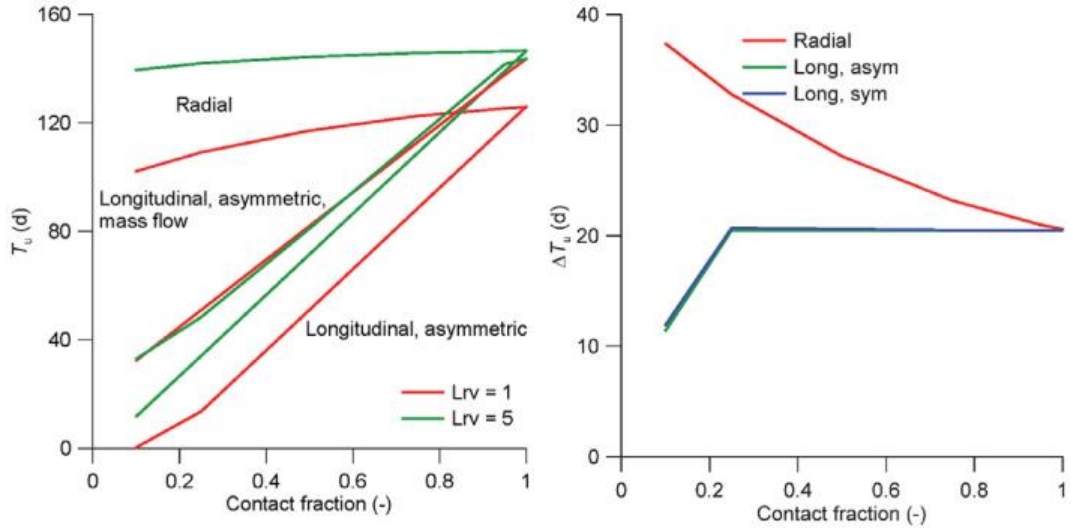

Fig. 9. The period of unconstrained uptake (T_u) for a nutrient like K with an adsorption constant of 10 mL cm^{-3}, an initial available amount of 225 kg ha^{-1}, and an uptake rate of 3 kg ha^{-1} d^{-1} for partial radial and longitudinal contact, the latter for asymmetrical and symmetrical position of contact area, as a function of the degree of partial contact (left) and the difference in T_u between root-length densities (L_{rv}) of 5 and 1 cm cm^{-3} (right).

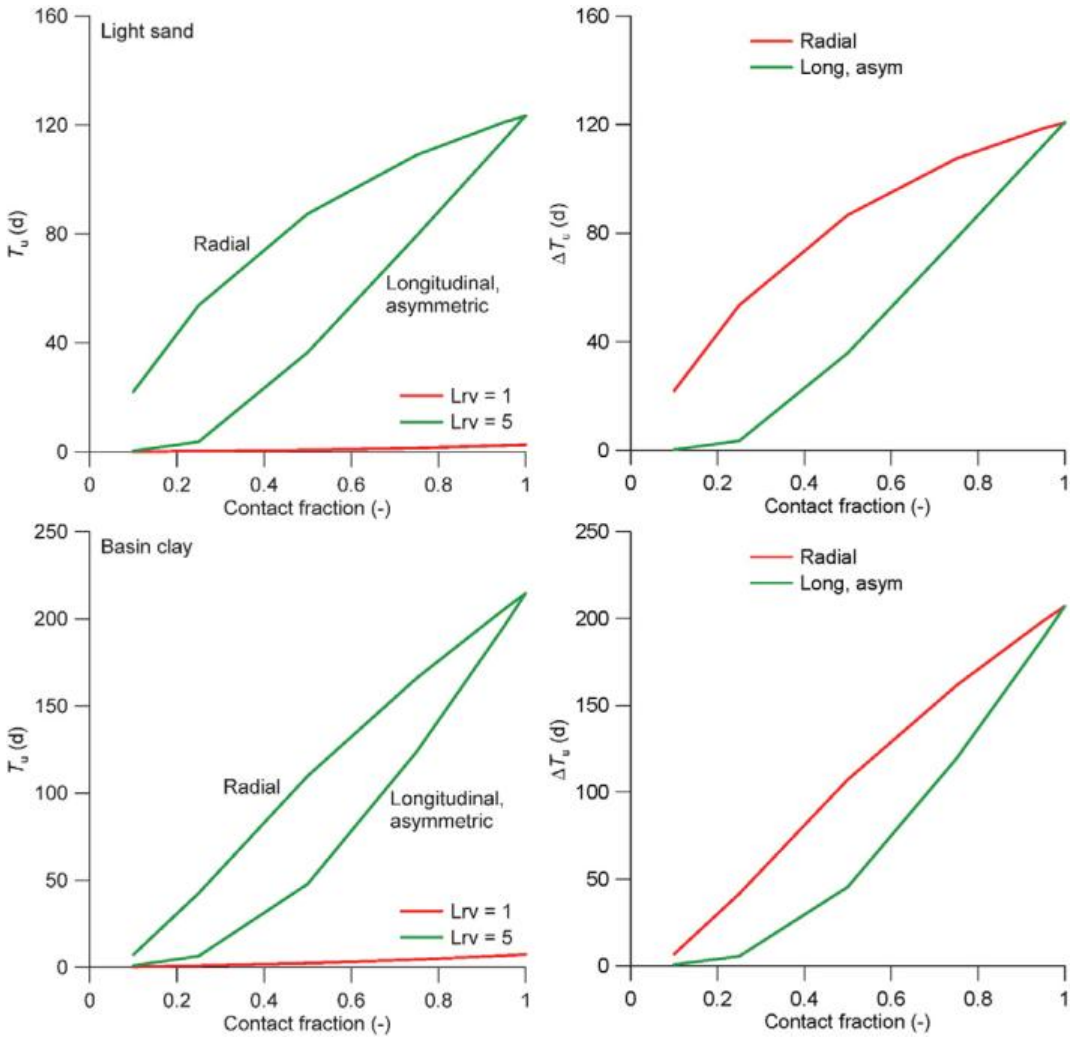

Fig. 10. The period of unconstrained uptake (T_u) for P and two soils, fine sand and basin clay (the nonlinear adsorption isotherms are given in Fig. 4) as a function of the degree of partial contact for radial and longitudinal asymmetrical contact (left) and the difference in T_u between root-length densities (L_{rv}) of 5 and 1 cm cm^{-3} (right).

Figure 11 is similar to Fig. 7 through 9, but here the uptake of water is considered. An increase in root-length density hardly leads to an increase in the period of unconstrained uptake.

Discussion

The first question formulated in the introduction (Can the analytical steady-rate solutions for nutrient and water uptake be adjusted, given cylinder geometry, to partial root–soil contact effects in either radial or longitudinal representations?) can be answered in the affirmative, as the steady-rate solution can be used for the pr situation. However, for the lr situation, this is not always the case because the limiting value can be reached before a steady-rate phase has developed. In case of linear adsorption, the analytical solution given in Eq. [37] can be used. For water and some nutrients (P), the steady-rate approach can be used. (See Fig. 10.8 in de Willigen and van Noordwijk, 1987a).

As to the second question (Is there a simple expression for the additional root-length density needed in a layer of soil to account for the more complex root–soil geometry through use of the standard model but with adjusted effective root-length density?), also a mixed answer can be given. It is clear that the pr situation with quantitatively the same surface in contact with the soil solution is more favorable than the lr situation. This has to do with the lower transport distances (Fig. 6 and 7). So one should expect that with partial radial contact a substantial increase in root-length density would result in a substantial increase in the length of the period of unconstrained uptake. However, as Fig. 8 shows, in the absence of adsorption and with a large amount of available nutrient, a fivefold increase in root-length density leads to a very modest increase in T_u. The value of the dimensionless $t_{u,max}$ is 2.10^4 and the rest term

$$\beta\rho^2\left(\frac{\ln\rho}{2}-\frac{3}{8}+\frac{1}{\psi_1}\sum_{k=1}^{\infty}\frac{\sin k\psi_1}{k^2}\right)$$

(see Eq. [27]) is, even at a partial contact of 0.1, <2% of $t_{u,max}$ for a root length density of 1 and ~0.3% for L_{rv} = 5; for contact of 0.9, the rest term is 0.6 and 0.06% for L_{rv} = 1 and 5, respectively. So even at low root density and low contact, T_u is close to its maximum value, and a fivefold increase in L_{rv} hardly increases T_u because of the low value of β(0.3). In the case of K, $t_{u,max}$ is 3.7×10^4, almost twice the value for NO_3, but for β = 10.3, the rest term is consequently larger; in the case of partial contact of 0.1, the ratio rest term/$t_{u,max}$ is 42 and 5.3% for L_{rv} = 1 and 5, respectively; for partial contact 0.9, the ratio is 12.5 and 4.2%. Figures 9 (right) and 10 (right) show that the effect of increased root-length density is considerably higher in the pr situation than in the lr situation. Figure 11 shows that also for water the effect of root-length density is almost negligible. This has to do with the high value of diffusivity in the range between the initial pressure head (−100 cm) and the limiting pressure head (approximately −5000 cm). The diffusivity in this range amounted to 350 to 1 and 1200 to 42 $cm^2\ d^{-1}$ for the sandy (B3) and the loamy (B13) soils, respectively.

For the basic situation, we mentioned the possibility of approximating the partial contact at a given root-length density with an effective root-length density and complete contact such that total contact was the same. An example is a root system with a root-length density of 1 cm cm^{-3} and a partial contact of 0.1 approximated by a root-length density of 0.1 cm cm^{-3} with complete contact. Again, Eq. [27] can be used (in the case of partial radial contact) to calculate t_u for both cases, and it appears that the approximation results in lower t_u both for NO_3 and K.

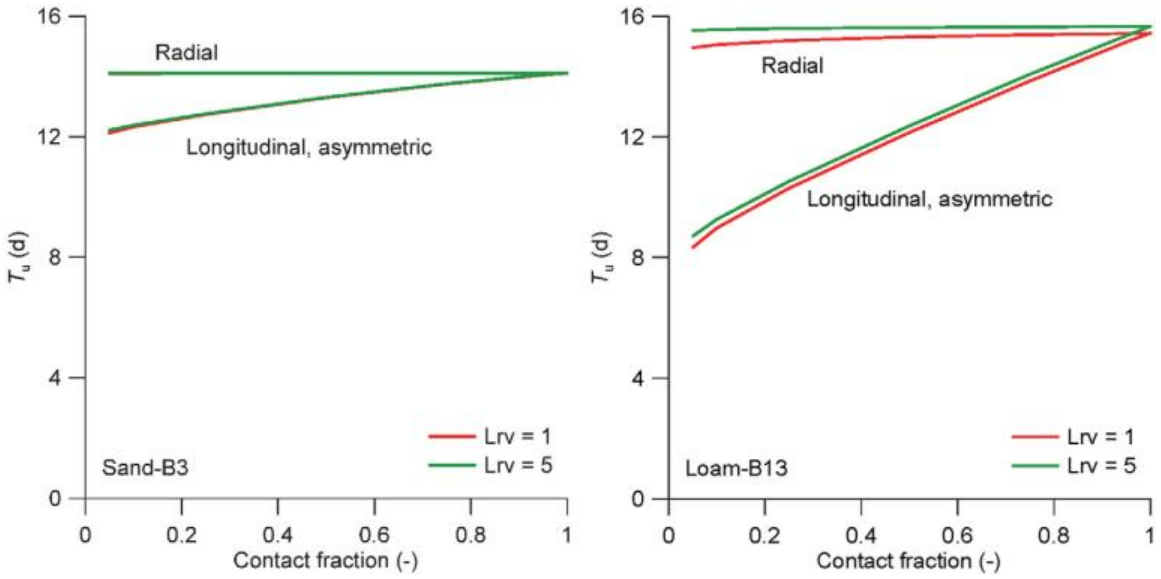

Fig. 11. The period of unconstrained uptake (T_u) for water and two soils with different hydraulic properties as a function of the degree of partial contact for radial and longitudinal asymmetrical contact (left) and the difference in T_u between root-length densities (L_{rv}) of 5 and 1 cm cm^{-3} (right).

All current 3-D models assume 100% root–soil contact and radial symmetry around roots while evaluating the consequences of mass flow plus diffusion for transport (Dunbabin et al., 2013). They avoid the assumption that all transport is directed toward the nearest root (as typically made in single-root models), but spatial resolution is limited and deviations from the uptake-shed assumption have not yet been convincingly demonstrated. It is likely that the partial contact situations considered here will lead to deviations from the Dirichlet tessellation of uptake-sheds based on distances to the nearest root, as actual transport pathways will differ from straight lines (as demonstrated by the streamlines in Fig. 6 and 7).

When two-dimensional cross-sections of 3-D root–soil realities are analyzed, the statistical distribution of angles with which roots intersect any plane can be estimated from the ratio of the maximum and minimum diameters of the root intersection (van Noordwijk et al., 1992). Deviations from a uniform distribution of angles (anisotropy) matter for estimates of root-length density from intersection density in two-dimensional maps, but the effects are small if point densities on mutually perpendicular planes are averaged.

The two contact situations considered here are the two extremes of the way partial root–soil contact interacts with uptake. The reality of root systems developing in aggregated, structured soils will probably be in between these two geometries. Results for the radial case (Fig. 12, left) show that uptake potential of roots is higher than that for roots with full contact at a density corrected for the percentage contact. The results for the longitudinal case (Fig. 12, right), in contrast, show a reduction in uptake potential more than proportional to the percentage contact. For mixed contact situations, multiplying root length density with contact fraction is possibly acceptable as an approximation. This comes on top of a correction for the irregular distribution of roots (as quantified in the root position effectivity ratio R_{per} of van Noordwijk, 1992) but is probably compensated by the ability of root systems to preferentially branch near locally enriched parts of the soil, with the strength of the local response dependent on current nutrient deficiencies in the plant as a whole. Where the focus is on a quantitative understanding of the soil nutrient supply situations where plant nutrient uptake is not growth limiting, measured root-length density (corrected for mycorrhizal hyphae) remains the primary parameter of interest, with the complexities of actual root–soil geometry as secondary modifiers.

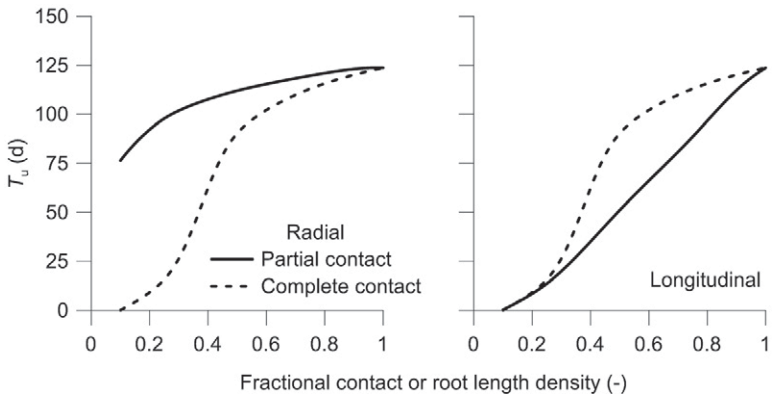

Fig. 12. The period of unconstrained uptake of the radial (left) or longitudinal (right) situation for partial and complete contact. The *x* axis gives fractional contact in the case of partial contact, with a root-length density of 1 cm cm^{-3}, and root-length density in the case of complete contact. The nutrient parameters are those of K given for Fig. 9.

Incomplete root–soil contact is but one of several aspects that has so far been ignored in common models of water transport in the soil–plant continuum along with water storage in the plant xylem and coarse roots (capacitance effect) and hydraulic architecture of leaf system (inductance effect) (Zhuang et al., 2014). More comprehensive models are emerging and provide insights into the important role of plant configuration and hydraulic heterogeneity in helping plants survive an adverse environment. As reviewed by dos Santos et al. (2017), in an update from earlier reviews of one-, two-, and three-dimensional models by Vrugt et al. (2001), detailed physical models describing root water uptake are an important tool for the prediction of soil water dynamics and crop transpiration, but the hydraulic parameters involved are hardly ever available, making them less attractive for many studies. A range of simpler empirical models keep track of the soil water balance but differ in (i) how root water uptake is partitioned over depth (with compensation in wetter soil layers for reduced uptake elsewhere in the root system) and (ii) how the transpiration reduction function is defined that slows down uptake from dry soil. Physical considerations of root–soil contact are relevant for the first case if contact varies with depth and in the second case if shrinking roots would lose soil contact in layers that still have plant-available water.

In their review of the complex, 3-D, and highly dynamic habitat offered by pores in the vadose zone, Hallett et al. (2013) called for a more process-based understanding of how biological processes affect the physical properties of soil across spatial scales and time that goes beyond descriptions of the complexity. Starting from roots as (part of) live organisms with high phenotypic plasticity and genetic selection on the effectiveness of the feedback loops can help in this respect. Our equations indicate the increases in root-length density needed in realistic geometries to achieve the same uptake as the idealized simple root geometry models predict. In many situations, this increase is within the existing error and uncertainty of root measurements in the field.

Thus, the consequences for water and nutrient uptake of partial root–soil contact of the type found where roots grow into a preexisting void larger than their own diameter will be small, especially if root hairs can be expected to develop to compensate for partial contact. It may be justified to ignore the associated complications for transport

pathways close to roots, as is commonly done in existing 3-D models. In contrast, the type of partial contact that arises when roots penetrate soil aggregates but traverse voids between them will generally not be negligible, but impacts on uptake can, for the radial contact situation, be bounded by a reduction of effective root length to the part in (full) contact with soil.

Conclusions

The consequences for water and nutrient uptake of partial root–soil contact of the type found where roots grow into a preexisting void larger than their own diameter will be small, especially if root hairs can be expected to develop to compensate for partial contact. It may be justified to ignore the associated complications for transport pathways close to roots, as is commonly done in existing 3-D models. In contrast, the type of partial contact that arises when roots penetrate soil aggregates but traverse voids between them will generally not be negligible, but impacts on uptake can, for the radial contact situation, be bounded by a reduction of effective root length to the part in (full) contact with soil. Technical conclusions for use in further uptake models are that (i) the steady-rate solution for T_u can be applied to the situation of pr but is less applicable to lr even in the case of non-adsorbed nutrients like NO_3, and (ii) the steady-rate solution can also be applied in the case of pr for nonlinearly adsorbed nutrients and water.

References

Alameda, D., and R. Villar. 2009. Moderate soil compaction: Implications on growth and architecture in seedlings of 17 woody plant species. Soil Tillage Res. 103:325–331. doi:10.1016/j.still.2008.10.029

Altemüller, H.J., and T. Haag. 1983. Mikroskopische Untersuchungen an Maiswurzeln i/m ungestörten Bodenverband. Kali-Briefe 16:349–363.

Arvidsson, J., and I. Håkansson. 2014. Response of different crops to soil compaction: Short-term effects in Swedish field experiments. Soil Tillage Res. 138:56–63. doi:10.1016/j.still.2013.12.006

Athmann, M., T. Kautz, R. Pude, and U. Köpke. 2013. Root growth in biopores: Evaluation with in situ endoscopy. Plant Soil 371:179–190. doi:10.1007/s11104-013-1673-5

Baldwin, J.P., P.H. Nye, and P.B. Tinker. 1973. Uptake of solutes by multiple root systems from soil. Plant Soil 38:621–635. doi:10.1007/BF00010701

Bartholomeus, R.P., J.P.M. Witte, P.M. van Bodegom, J.C. van Dam, and R. Aerts. 2008. Critical soil conditions for oxygen stress to plant roots: Substituting the Feddes-function by a process-based model. J. Hydrol. 360:147–165. doi:10.1016/j.jhydrol.2008.07.029

Bayala, J., L.K. Heng, M. van Noordwijk, and S.J. Ouedraogo. 2008. Hydraulic redistribution study in two native tree species of agroforestry parklands of West African dry savanna. Acta Oecol. 34:370–378. doi:10.1016/j.actao.2008.06.010

Bengough, A.G., K. Loades, and B.M. McKenzie. 2016. Root hairs aid soil penetration by anchoring the root surface to pore walls. J. Exp. Bot. 67:1071–1078. doi:10.1093/jxb/erv560

Bouma, J. 2010. Implications of the knowledge paradox for soil science. Adv. Agron. 106:143–171. doi:10.1016/S0065-2113(10)06004-9

Campbell, G.S. 1985. Soil physics with BASIC. Elsevier, Amsterdam.

Campbell, G.S., 1991. Simulation of water uptake by plant roots. In: J. Hanks and J.T. Ritchie, editors, Modeling plant and soil systems. Agron. Monogr. 31. ASA, CSSA, and SSSA, Madison, WI. p. 273–285. doi:10.2134/agronmonogr31.c12

Carminati, A., and D. Vetterlein. 2013. Plasticity of rhizosphere hydraulic properties as a key for efficient utilization of scarce resources. Ann. Bot. 112:277–290. doi:10.1093/aob/mcs262

Carminati, A., D. Vetterlein, N. Koebernick, S. Blaser, U. Weller, and H.J. Vogel. 2013. Do roots mind the gap? Plant Soil 367:651–661. doi:10.1007/s11104-012-1496-9

Churchill, R.V. 1972. Operational mathematics. 3rd ed. McGraw-Hill–Kogakusha, Tokyo.

Claassen, N., and S.A. Barber. 1974. A method for characterizing the relation between nutrient concentration and flux into roots of intact plants. Plant Physiol. 54:564–568. doi:10.1104/pp.54.4.564

Darwin, C. 1888. The power of movement in plants. John Murray, London.

de Willigen, P., J.C. van Dam, M. Javaux, and M. Heinen. 2012. Root water uptake as simulated by three soil water flow models. Vadose Zone J. 11(3). doi:10.2136/vzj2012.0018

de Willigen, P., and M. van Noordwijk. 1984. Mathematical models on diffusion of oxygen to and within plant roots, with special emphasis on effects of soil–root contact: I. Derivations of the models. Plant Soil 77:215–231. doi:10.1007/BF02182925

de Willigen, P., and M. van Noordwijk. 1987a. Roots for plant production and nutrient use efficiency. Ph.D. thesis. Wageningen Agric. Univ., Wageningen, the Netherlands.

de Willigen, P., and M. van Noordwijk. 1987b. Uptake potential of non-regularly distributed roots. J. Plant Nutr. 10:1273–1280. doi:10.1080/01904168709363656

de Willigen, P., and M. van Noordwijk. 1989. Model calculations on the relative importance of internal longitudinal diffusion for aeration of roots of non-wetland plants. Plant Soil 113:111–119. doi:10.1007/BF02181928

de Willigen, P., and M. van Noordwijk. 1994a. Diffusion and mass flow to a root with constant nutrient demand or behaving as a zero-sink: I. Constant uptake. Soil Sci. 157:162–170. doi:10.1097/00010694-199403000-00004

de Willigen, P., and M. van Noordwijk. 1994b. Diffusion and mass flow to a root with constant nutrient demand or behaving as a zero-sink: II. Zero-sink uptake. Soil Sci. 157:171–175. doi:10.1097/00010694-199403000-00005

dos Santos, M.A., Q. de Jong van Lier, J.C. van Dam, and A.H.F. Bezerra. 2017. Benchmarking test of empirical root water uptake models. Hydrol. Earth Syst. Sci. 21:473–493. doi:10.5194/hess-21-473-2017

Dunbabin, V.M., J.A. Postma, A. Schnepf, L. Pagès, M. Javaux, L. Wu, et al. 2013. Modelling root–soil interactions using three–dimensional models of root growth, architecture and function. Plant Soil 372:93–124. doi:10.1007/s11104-013-1769-y

Faiz, S.M.A., and P.E. Weatherley. 1978. Further investigations into the location and magnitude of the hydraulic resistances in the soil–plant system. New Phytol. 81:19–28. doi:10.1111/j.1469-8137.1978.tb01599.x

Haling, R.E., L.K. Brown, A.G. Bengough, I.M. Young, P.D. Hallett, P.J. White, and T.S. George. 2013. Root hairs improve root penetration, root–soil contact, and phosphorus acquisition in soils of different strength. J. Exp. Bot. 64:3711–3721. doi:10.1093/jxb/ert200

Hallett, P.D., K.H. Karim, A.G. Bengough, and W. Otten. 2013. Biophysics of the vadose zone: From reality to model systems and back again. Vadose Zone J. 12(4). doi:10.2136/vzj2013.05.0090

Han, E., T. Kautz, U. Perkons, D. Uteau, S. Peth, N. Huang, et al. 2015. Root growth dynamics inside and outside of soil biopores as affected by crop sequence determined with the profile wall method. Biol. Fertil. Soils 51:847–856. doi:10.1007/s00374-015-1032-1

Herkelrath, W.N., E.E. Miller, and W.R. Gardner. 1977. Water uptake by plants: II. The root contact model. Soil Sci. Soc. Am. J. 41:1039–1043. doi:10.2136/sssaj1977.03615995004100060004x

Jenny, H., and K. Grossenbacher. 1963. Root–soil boundary zones as seen in the electron microscope. Soil Sci. Soc. Am. J. 27:273–277. doi:10.2136/sssaj1963.03615995002700030018x

Kautz, T., and U. Köpke. 2010. In situ endoscopy: New insights to root growth in biopores. Plant Biosyst. 144:440–442. doi:10.1080/11263501003726185

Kooistra, M.J., D. Schoonderbeek, F.R. Boone, B.W. Veen, and M. van Noordwijk. 1992. Root–soil contact of maize, as measured by a thin-section technique. Plant Soil 139:119–129. doi:10.1007/BF00012849

Kooistra, M.J., and M. van Noordwijk. 1996. Soil architecture and distribution of organic carbon. In: M.R. Carter and B.A. Stewart, editors, Structure and organic carbon storage in agricultural soils. Advances in Soil Science. CRC Press, Boca Raton, FL. p. 15–57.

Kremer, C., C.O. Stöckle, A.R. Kemenian, and T. Howell. 2008. A canopy transpiration and photosynthesis model for evaluating simple crop productivity models. In: L.R. Ahuja et al., editors, Response of crops to limited water: Understanding and modeling water stress effects on plant growth processes. Adv. Agric. Syst. Model. 1. ASA, CSSA, and SSSA, Madison, WI. p. 165–189.

Liu, X.P., W.J. Zhang, X.Y. Wang, Y.J. Cai, and J.G. Chang. 2015. Root–soil air gap and resistance to water flow at the soil–root interface of *Robinia pseudoacacia*. Tree Physiol. 35:1343–1355.

doi:10.1093/treephys/tpv075

Metselaar, K., and Q. de Jong van Lier. 2011. Scales in single root water uptake models: A review, analysis and synthesis. Eur. J. Soil Sci. 62:657–665. doi:10.1111/j.1365-2389.2011.01385.x

Neumann, R.B., and Z.G. Cardon. 2012. The magnitude of hydraulic redistribution by plant roots: A review and synthesis of empirical and modeling studies. New Phytol. 194:337–352. doi:10.1111/j.1469-8137.2012.04088.x

North, G.B., and P.S. Nobel. 1997. Root–soil contact for the desert succulent *Agave deserti* in wet and drying soil. New Phytol. 135:21–29. doi:10.1046/j.1469-8137.1997.00620.x

Nye, P.H., and P.B. Tinker. 1977. Solute movement in the soil–root system. Univ. of California Press, Oakland.

Raats, P.A.C. 1970. Steady infiltration from line sources and furrows. Soil Sci. Soc. Am. Proc. 34:709–714. doi:10.2136/sssaj1970.03615995003400050015x

Rappoldt, C. 1992. Diffusion in aggregated soil. Ph.D. thesis. Wageningen Agricultural Univ., Wageningen, the Netherlands.

Schmidt, S., A.G. Bengough, P.J. Gregory, D.V. Grinev, and W. Otten. 2012. Estimating root–soil contact from 3D X-ray microtomographs. Eur. J. Soil Sci. 63:776–786. doi:10.1111/j.1365-2389.2012.01487.x

Tracy, S.R., C.R. Black, J.A. Roberts, and S.J. Mooney. 2011. Soil compaction: A review of past and present techniques for investigating effects on root growth. J. Sci. Food Agric. 91:1528–1537. doi:10.1002/jsfa.4424

van Noordwijk, M. 1992. Root position effectivity ratio, Rper: A simple measure of the effects of non-homogeneous root distribution on uptake of homogeneous resources. In: L. Kutschera et al., editors, Root ecology and its practical application: 3rd ISRR Symposium, Vienna. 2–6 Sept. 1991. Verein fur Wurzeinforschung, Klagenfurt, Austria. p. 790–792.

van Noordwijk, M., and G. Brouwer. 1993. Gas-filled root porosity in response to temporary low oxygen supply in different growth stages. Plant Soil 152:187–199. doi:10.1007/BF00029088

van Noordwijk, M., G. Brouwer, and K. Harmanny. 1993b. Concepts and methods for studying interactions of roots and soil structure. Geoderma 56:351–375. doi:10.1016/0016-7061(93)90122-2

van Noordwijk, M., G. Brouwer, F. Meijboom, G. do Rosario, and M. Oliveira, and A.G. Bengough. 2000. Trench profile techniques and core break methods. In: A.L. Smit et al, editors, Root methods: A handbook. Springer, Berlin. p. 211–233.

van Noordwijk, M., and P. de Willigen. 1984. Mathematical models on diffusion of oxygen to and within plant roots, with special emphasis on effects of soil–root contact: II. Applications. Plant Soil 77:233–241. doi:10.1007/BF02182926

van Noordwijk, M., P. de Willigen, P.A.I. Ehlert, and W.J. Chardon. 1990. A simple model of P uptake by crops as a possible basis for P fertilizer recommendations. Neth. J. Agric. Sci. 38:317–332.

van Noordwijk, M., M.J. Kooistra, F.R. Boone, B.W. Veen, and D. Schoonderbeek. 1992. Root–soil contact of maize, as measured by a thin-section technique. Plant Soil 139:109–118. doi:10.1007/BF00012848

van Noordwijk, M., D. Schoonderbeek, and M.J. Kooistra. 1993a. Root–soil contact of field-grown winter wheat. Geoderma 56:277–286. doi:10.1016/0016-7061(93)90117-4

Veen, B.W., M. van Noordwijk, P. de Willigen, F.R. Boone, and M.J. Kooistra. 1992. Root–soil contact of maize, as measured by a thin-section technique. Plant Soil 139:131–138. doi:10.1007/BF00012850

Vrugt, J.A., M.T. van Wijk, J.W. Hopmans, and J. Šimunek. 2001. One-, two-, and three-dimensional root water uptake functions for transient modeling. Water Resour. Res. 37:2457–2470. doi:10.1029/2000WR000027

White, R.G., and J.A. Kirkegaard. 2010. The distribution and abundance of wheat roots in a dense, structured subsoil: Implications for water uptake. Plant Cell Environ. 33:133–148. doi:10.1111/j.1365-3040.2009.02059.x

Wösten, J.H.M., G.J. Veerman, W.J.M. de Groot, and J. Stolte. 2001. Waterretentie- en doorlatendheidskarakteristieken van boven- en ondergronden in Nederland: De Staringreeks. Vernieuwde uitgave. Alterra-rapport 153. Alterra, Wageningen, the Netherlands. http://edepot.wur.nl/43272

Young, I.M. 1998. Biophysical interactions at the root–soil interface: A review. J. Agric. Sci. 130:1–7. doi:10.1017/S002185969700498X

Zhuang, J., G.R. Yu, and K. Nakayama. 2014. A series RCL circuit theory for analyzing non-steady-state water uptake of maize plants. Sci. Rep. 4:6720. doi:10.1038/srep06720